



Master's Thesis

Master in Telecommunication Engineering

H- α decomposition and unsupervised Wishart
classification for dual-polarized polarimetric
SAR data

Joan Domènech Olivie

Supervisor: Marc Bara Iniesta

Department of Telecommunications and Systems Engineering

**Escola Tècnica Superior d'Enginyeria (ETSE)
Universitat Autònoma de Barcelona (UAB)**

January 2015

El sotasignant, Marc Bara Iniesta, Professor de l'Escola Tècnica Superior d'Enginyeria (ETSE) de la Universitat Autònoma de Barcelona (UAB),

CERTIFICA:

Que el projecte presentat en aquesta memòria de Treball Final de Master ha estat realitzat sota la seva direcció per l'alumne Joan Domènech Olivé.

I, perquè consti a tots els efectes, signa el present certificat.

Bellaterra, 20 de Gener del 2015.



Signatura: Marc Bara Iniesta

Resum:

En aquesta tesi s'ha aplicat el mètode de descomposició H- α juntament amb el classificador Wishart a un conjunt real de dades SAR (Synthetic Aperture Radar) utilitzant l'entorn MATLAB. El conjunt de dades va ser capturat a través del satèl·lit TerraSAR-X i correspon a la regió de Pangkalan Bun, a Indonèsia. L'objectiu de la tesi és analitzar i avaluar la precisió del classificador. S'ha pogut comprovar que les imatges SAR es poden segmentar utilitzant les propietats dels mecanismes de dispersió caracteritzats pels paràmetres d'entropia i alpha. Per tant, s'ha obtingut una bona segmentació de les diferents zones de la imatge a partir dels paràmetres d'entropia i alpha en combinació amb el classificador Wishart.

Resumen:

En esta tesis se ha aplicado el método de descomposición H- α junto con el clasificador Wishart a un conjunto real de datos SAR (Synthetic Aperture Radar) utilizando el MATLAB. El conjunto de datos fue capturado a través del satélite TerraSAR-X y corresponde a la región de Pangkalan Bun, en Indonesia. El objetivo de la tesis es analizar y evaluar la precisión del clasificador. Se ha podido comprobar que las imágenes SAR se pueden segmentar utilizando las propiedades de los mecanismos de dispersión caracterizados por los parámetros de entropía y alpha. Por lo tanto, se ha obtenido una buena segmentación de las distintas zonas de la imagen a partir de los parámetros de entropía y alpha en combinación con el clasificador Wishart.

Summary:

In this thesis the H- α decomposition method and the unsupervised Wishart classifier have been applied to a dual-polarized polarimetric Synthetic Aperture Radar (SAR) dataset using MATLAB computing environment. The dataset was captured by TerraSAR-X satellite and corresponds to the region of Pangkalan Bun, Indonesia. The objective is to analyze and evaluate the precision of the classification. It has been proved that the SAR image can be segmented taking advantage of the properties of the scattering mechanism characterized by the entropy and alpha parameters. Hence, a robust segmentation of the different zones of the image has been obtained by means of the entropy and alpha parameters in combination with the Wishart classifier.

Table of Contents

1. Introduction	9
2. SAR fundamentals	11
2.1. Introduction to SAR	11
2.2. Geometry of SAR system	12
2.3. Range resolution	13
2.4. Azimuth resolution	14
2.5. Modes of operation	16
3. Polarimetric SAR analysis	18
3.1. Polarization state of electromagnetic waves	18
3.2. Polarization in SAR systems	20
3.3. Jones vector	22
3.4. Scattering or Sinclair matrix	23
3.5. Coherency matrix	25
4. Indonesia Case Study description	27
4.1. TerraSAR-X spacecraft	27
4.2. TerraSAR-X delivery file format	29
4.3. Description of the Indonesia dataset	30
5. H- α Decomposition applied to the Case Study	33
5.1. Theory of H- α Decomposition	33
5.1.1. Extraction of the H- α parameters	34
5.1.2. Interpretation of H- α feature space	35
5.2. Application of H- α Decomposition to the Case Study	37
5.3. Decomposition results of the Case Study	37

6. Wishart classifier applied to the Case Study	46
6.1. Supervised and unsupervised terrain classification	46
6.2. Wishart classifier algorithm	47
6.3. Application of the Wishart classifier to the Case Study	48
6.4. Classification results of the Case Study	49
7. Conclusions	58
References	60

List of Tables

Table 1. Jones vectors and the corresponding polarization ellipse parameters for some canonical polarization states	23
Table 2. Main parameters of TerraSAR-X satellite	27
Table 3. Processing levels of TerraSAR-X satellite	29
Table 4. Characteristics of the TerraSAR-X Indonesia dataset	30
Table 5. Zones of H- α feature space	36

List of Figures

Fig. 1.	Side-looking geometry of a monostatic SAR system	12
Fig. 2.	Geometric representation of slant range and ground range resolution Azimuth resolution	13
Fig. 3.	Geometric representation of azimuth resolution	14
Fig. 4.	Stripmap mode	16
Fig. 5.	Spotlight mode	16
Fig. 6.	ScanSAR mode	17
Fig. 7.	Electric field of linear or plane polarization	18
Fig. 8.	Electric field of circular polarization	19
Fig. 9.	Polarization ellipse	20
Fig. 10.	Artist view of TerraSAR-X satellite	28
Fig. 11.	Map of the area covered by the Case Study dataset	30
Fig. 12.	Reconstruction image of the entire dataset and HH channels of the three selected subsets	31
Fig. 13.	Aerial image of the three subsets captured by Google Earth and their corresponding HH channel matrix image	32
Fig. 14.	H- α classification plane	35
Fig. 15.	Overall data flow diagram for the Case Study	37
Fig. 16.	Polarimetric channels of the subset A: (a) HH-channel, (b) VV-channel	37
Fig. 17.	Polarimetric channels of the subset A with 5x5 multilook window: (a) HH-channel, (b) VV-channel	38
Fig. 18.	Parameters extracted from the subset A: (a) entropy, (b) alpha angle	39
Fig. 19.	Zoom of the zones with the highest alpha in subset A produced by the yellow buildings	40
Fig. 20.	H- α plane of the subset A: (a) zones with diferent colors, (b) density plot of the plane	40
Fig. 21.	Subset A classified using H- α plane: (a) subset A, (b) area of subset A in detail	41

Fig. 22.	Parameters extracted from the subset B: (a) entropy, (b) alpha angle	41
Fig. 23.	H- α plane of the subset B: (a) zones with diferent colors, (b) density plot of the plane	42
Fig. 24.	Subset B classified using H- α plane	43
Fig. 25.	Parameters extracted from the subset C: (a) entropy, (b) alpha angle	43
Fig. 26.	H- α plane of the subset C: (a) zones with diferent colors, (b) density plot of the plane	44
Fig. 27.	Subset C classified using H- α plane: (a) subset C, (b) area of subset C in detail	44
Fig. 28.	Data flow diagram of the Wishart classifier	48
Fig. 29.	Cluster centers of the initial classification map of the subset A	49
Fig. 30.	First iteration of the subset A: (a) classified image, (b) cluster centers	50
Fig. 31.	Second iteration of the subset A: (a) classified image, (b) cluster centers	50
Fig. 32.	Third iteration of the subset A: (a) classified image, (b) cluster centers	51
Fig. 33.	Cluster centers of the initial classification map of the subset B	52
Fig. 34.	First iteration of the subset B: (a) classified image, (b) cluster centers	52
Fig. 35.	Second iteration of the subset B: (a) classified image, (b) cluster centers	53
Fig. 36.	Third iteration of the subset B: (a) classified image, (b) cluster centers	54
Fig. 37.	Cluster centers of the initial classification map of the subset C	54
Fig. 38.	First iteration of the subset C: (a) classified image, (b) cluster centers	55
Fig. 39.	Second iteration of the subset C: (a) classified image, (b) cluster centers	56
Fig. 40.	Third iteration of the subset C: (a) classified image, (b) cluster centers	56

Chapter 1

Introduction

Broad-area high-resolution imaging is required many times in environmental monitoring, military systems, earth-resource mapping, surface deformation detection and disasters monitoring (forest fires, floods and oil spills), among others. Sometimes this imagery must be acquired in adverse situations, at night or during inclement weather. Synthetic Aperture Radar (SAR) provides such a capability, taking advantage of the long-range propagation characteristics of radar signals and the complex information processing capability to provide high-resolution imagery [1].

Traditional SAR systems were mainly operated on single-polarization mode, but nowadays the technological advancements allowed developing and operating SAR systems with multi polarization observation capability. The usage of multi polarization data has increased further the ability of extracting physical quantities of the scattering targets [2]. Quad polarization data have several advantages but the high operational cost and system constraints of full-polarization SAR systems make more common the usage of the single and dual-polarization. Although there are many platforms that can be operated on quad polarization mode, they are more often operating on single or dual-polarization mode instead.

Polarimetric decompositions are techniques used to generate polarimetric discriminators that can be used for analysis, interpretation and classification of SAR data [3]. These techniques allow the information extraction of the scattering processes that involve a specified target. H- α decomposition is an entropy based decomposition method based on the hypothesis that the polarization scattering characteristics can be represented by the space of the entropy and the averaged scattering angle α by means of the eigenvalue analysis of Hermitian matrices.

Terrain and land-use classifications are probably the most important applications of polarimetric synthetic aperture radar (PolSAR). In this thesis an algorithm proposed by Lee et al. has been developed in MATLAB computing environment, which is a combination of the unsupervised H- α decomposition classifier and the supervised Wishart classifier.

Chapter 2

SAR fundamentals

2.1 Introduction to SAR

Synthetic Aperture Radar (SAR) is based on the generation of an effective long antenna by signal-processing means rather than by the use of a long physical antenna [4]. Only a single and relatively small physical antenna is used in most cases and this is enough to acquire high resolutions. SAR uses a single beam-forming antenna carried on a moving platform, which can be an aircraft or a satellite. The platform travels along a path transmitting microwave pulses towards the ground. Some of the transmitted microwave energy is reflected back towards the sensor where it is received as a signal. The received signal is first pre-processed, involving demodulation, to create the row data and then is processed applying image formation algorithms to obtain a reflectivity map image. Hence, SAR obtains high resolutions simulating a real aperture by integrating the pulse echos into a composite signal. It is possible after applying appropriate processing to simulate effective antenna lengths up to 100 m or more [5].

Since SAR works in the microwave region of the electromagnetic spectrum, usually between P-band and Ka-band [6], it avoids weather-related limitations like cloud-cover or rainfall. So, it achieves equally good results in all weather conditions and also is independent of lighting conditions, acquiring accurate data at day or night.

In the last years, SAR technology has improved and the data collection has achieved high reliability and quality, so the demand for using SAR in a variety of applications is increasing. It has military applications and earth-science related applications such as mapping and

monitoring vegetation and sea-ice, terrain classification, finding minerals and evaluation of environmental damages, among others. Currently, the coverage rates of an airborne SAR system are capable of exceeding $1 \text{ km}^2/\text{s}$ at a resolution of 1 m^2 , thus producing over one million pixels each second [7].

2.2 Geometry of SAR system

The side-looking geometry of a monostatic SAR system is shown in Figure 1. The SAR sensor borne on a satellite platform flies over the territory that is sensed at a certain velocity, illuminating with pulses of electromagnetic radiation the Earth surface perpendicular to the flight line direction [8].

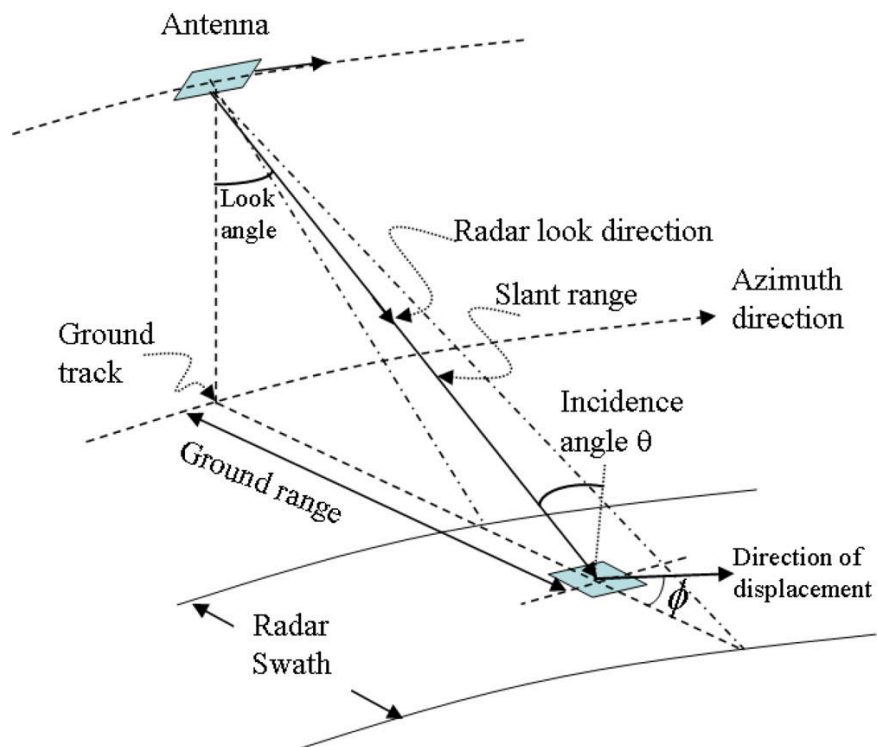


Fig. 1. Side-looking geometry of a monostatic SAR system

The direction of travel of the platform is referred to as the *azimuth* or *along-track* direction. The distance from the sensor to the ground is the *slant range*. *Ground range* refers to the across-track dimension perpendicular to the flight direction [9]. The angle from which the satellite observes the surface is the *look angle*. The *incidence angle* θ relates the direction of the radar pulses towards the normal vector of the terrain. The incidence angle is commonly used to describe the angular relationship between the radar beam and the ground, surface layer or a target [10].

The antenna beam of a side-looking radar is directed perpendicular to the flight path and illuminates a swath parallel to the platform ground track. The *radar swath* is the width of the imaged scene in the range dimension, so it refers to the strip of the Earth's surface from which data are collected by the radar. The portion of the image swath closest to the nadir track of the radar platform is called the *near range* while the portion of the swath farthest from the nadir is called the *far range* [11].

2.3 Range resolution

Range resolution is the ability of the radar system to distinguish between two or more targets on the same bearing but at different ranges [12]. Pulse width is the primary factor in range resolution. For a single frequency waveform, short pulses mean a fine range resolution but at the same time it is important that these short pulses have high energy to enable the detection of the reflected signals in order to obtain a good value of signal-to-noise ratio (SNR). This is accomplished by using pulse compression techniques. These techniques consist of emitting pulses that are linearly modulated in frequency for a duration of time T_p [13]. The frequency of the signal, called *chirp*, sweeps a band B and it is centered on a carrier at frequency f_0 . The received signal is then processed with a matched filter that compresses the long pulse to an effective duration equal to $1/B$. Range resolution is also dependent of the look angle but independent of the height of the antenna to the surface.

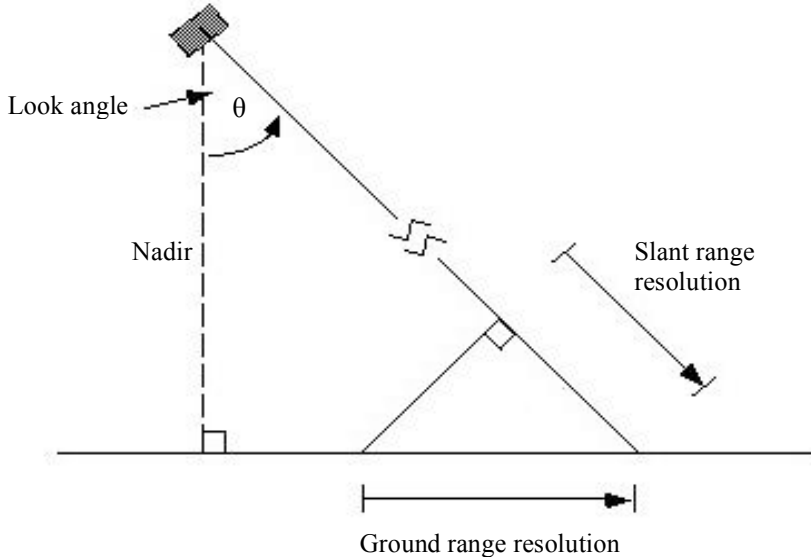


Fig. 2. Geometric representation of slant range and ground range resolution

The ground range resolution δx is the change in ground range associated with a slant range resolution of δr and is given by (1).

$$\delta x = \frac{\delta r}{\sin\theta} \quad (1)$$

where θ is the incidence angle and δr is given by (2).

$$\delta r = \frac{c}{2B} \quad (2)$$

where c is the speed of light and $1/B$ is the effective duration of the pulse. Hence, according to the formulas, a well-designed radar system with maximum efficiency should be able to distinguish targets separated by one-half the pulse width time. This way the echoes received do not overlap.

2.4 Azimuth resolution

Azimuth resolution is the minimum distance on the ground in the direction parallel to the flight path of the aircraft at which two targets can be separately imaged [4]. Azimuth resolution is dependent on aperture length and radar wavelength. The longitude of a SAR antenna is synthesized corresponding to the amount of time that the target remains illuminated while the sensor is flying overhead. This way the resolution of the azimuth direction is improved since a large antenna aperture is simulated.

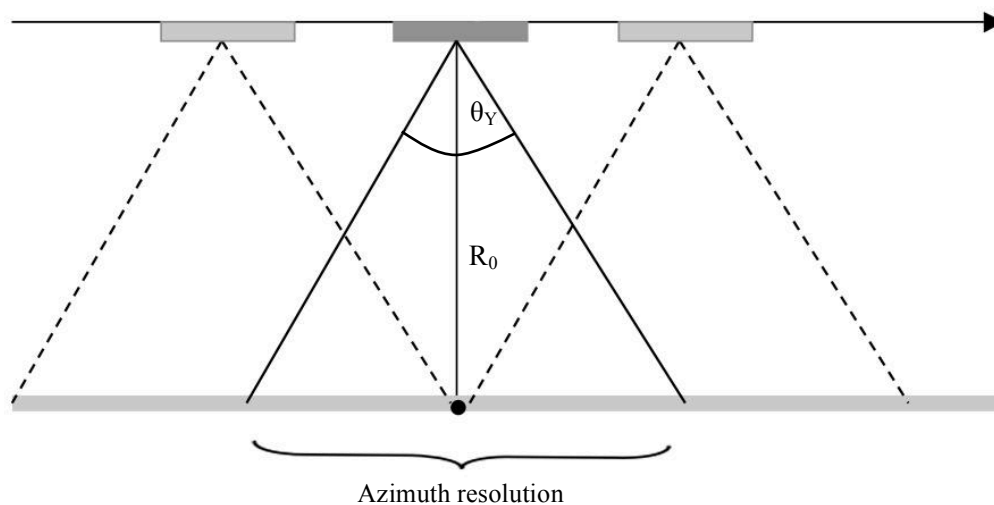


Fig. 3. Geometric representation of azimuth resolution

Two targets in the azimuth or along-track resolution can be separated only if the distance between them is larger than the radar beamwidth [14], so they cannot be in the radar beam at the same time.

The azimuth resolution for a real antenna with a beam width θ_Y at range R_0 is given by (3).

$$\delta y = R_0 \theta_Y \quad (3)$$

Taking into account that the antenna beam width is proportional to the aperture size [15],

$$\theta_Y \approx \frac{\lambda}{L_Y} \quad (4)$$

where L_Y refers to the physical dimensions of the real antenna aperture along the azimuth direction and λ is the wavelength corresponding to the carrier frequency of the transmitted signal. So, the azimuth resolution results in (5).

$$\delta y = \frac{R_0 \lambda}{L_Y} \quad (5)$$

It is observed, according to the formula, that high resolution in azimuth requires large antennas. In order to achieve high resolution the concept of synthetic aperture is applied. The resulting synthetic beam width is (6) [16].

$$\theta_Y = \frac{L_Y}{2 \cdot R_0} \quad (6)$$

So, the corresponding azimuth resolution for a synthetic aperture antenna when the scatterer is coherently integrated along the flight track results in (7).

$$\delta y = \frac{L_Y}{2} \quad (7)$$

It is observed that the azimuth resolution is dependent only of the physical size of the real antenna and independent of the range or wavelength.

2.5 Modes of operation

In SAR operations there are generally three imaging modes for data collection; they are stripmap mode, spotlight mode and scanSAR mode [17].

- Stripmap mode:

In this mode the ground swath is illuminated with a continuous sequence of pulses while the antenna pointing is fixed in elevation and azimuth relative to the flight line (usually normal to the flight line) [18]. The data acquired is an image strip with continuous image quality in azimuth and follows the length contour of the flight line of the platform itself. This mode is usually used for the mapping of large areas of terrain.

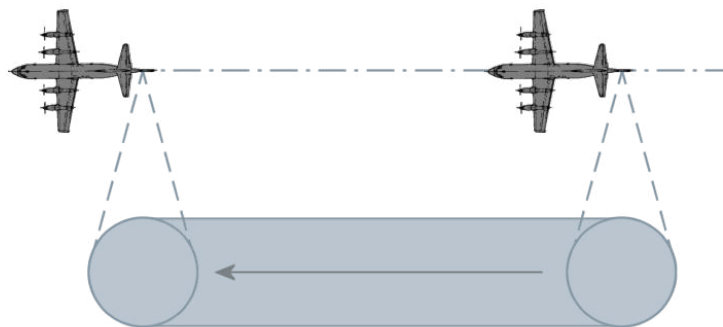


Fig. 4. Stripmap mode

- Spotlight mode:

During the observation of a particular ground scene the radar beam is steered so that the predetermined area of interest is continuously illuminated while the aircraft flies by in a straight line; hence the synthetic aperture becomes larger [19].

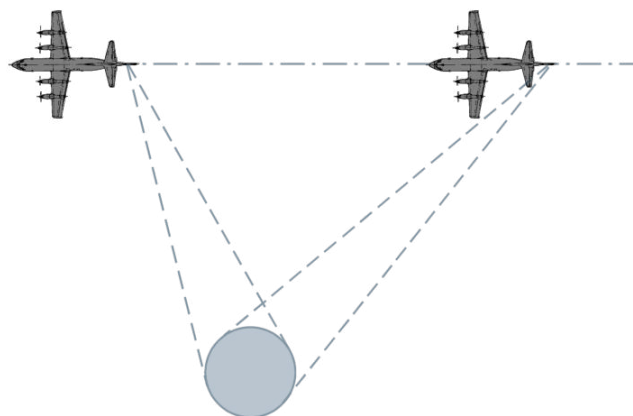


Fig. 5. Spotlight mode

This mode is capable of extending the high-resolution SAR imaging capability significantly since when more pulses are used, the azimuth resolution is increased. In spotlight mode the spatial coverage is reduced, since other areas within a given accessibility swath of the SAR cannot be illuminated while the radar beam is spotlighting over a particular target area.

- ScanSAR mode:

This mode achieves a wider imaged swath by scanning several adjacent ground sub-swaths with simultaneous beams, each with a different incidence angle [20]. ScanSAR mode provides large area coverage at the expense of azimuth resolution.

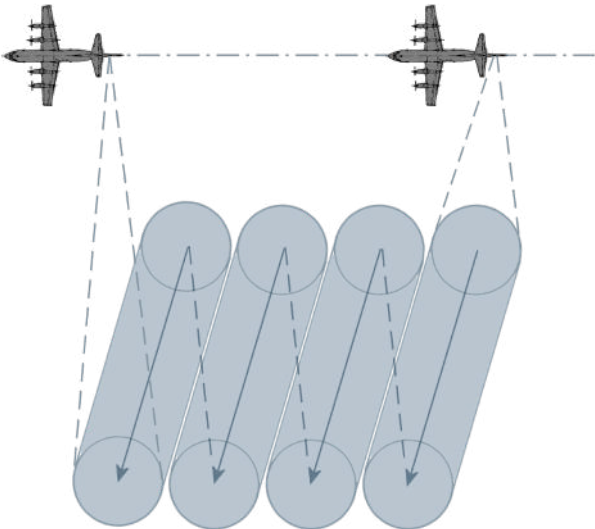


Fig. 6. ScanSAR mode

Chapter 3

Polarimetric SAR analysis

3.1 Polarization state of electromagnetic waves

Electromagnetic waves are formed when an electric field couples with a magnetic field. The magnetic and electric fields of an electromagnetic wave are perpendicular to each other and to the direction of the wave. For a plane electromagnetic wave, polarization refers to the locus of the electric field vector in the plane perpendicular to the direction of propagation [21]. The polarization is described by the geometric figure traced by the electric field vector upon a stationary plane perpendicular to the direction of propagation, as the wave travels through that plane [22].

Most of the polarized radars use two orthogonal linearly polarized antennas; hence the Cartesian coordinate system is used as in Figure 7.

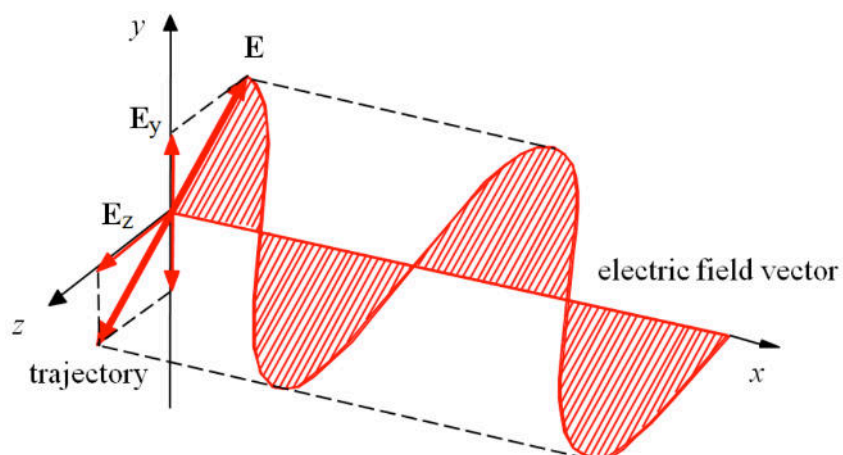


Fig. 7. Electric field of linear or plane polarization

In Figure 7, x indicates the direction of wave propagation and the corresponding electric field is located in y - z plane and E_y and E_z are the y -component and z -component of the electric field vector E respectively. The figure shows a linear polarization of an electromagnetic wave. If the oscillation of the electric field vector is observed from behind toward the propagation direction in x -axis, the trajectory becomes a line on y - z plane. The polarization is vertical when the electric lines of force lie in a vertical direction and is horizontal when the electric lines of force lie in a horizontal direction.

Electromagnetic wave propagation of circular polarization is illustrated in Figure 8. Circular polarization has the electric lines of force rotating through 360 degrees with every cycle of energy [23].

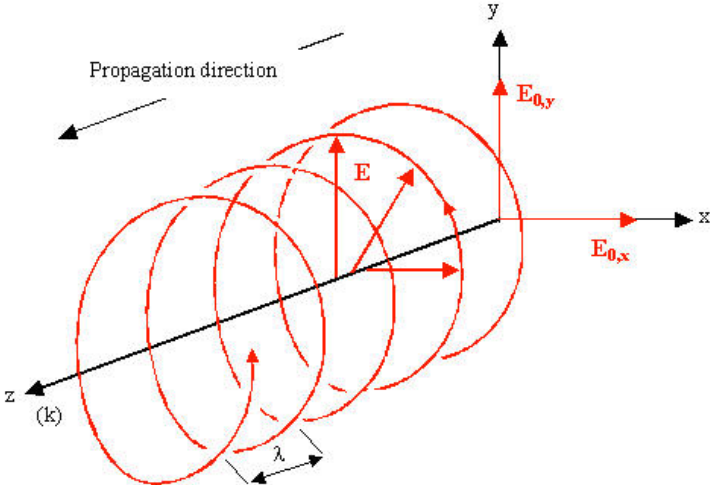


Fig. 8. Electric field of circular polarization

The amplitudes of the y -component and z -component of the electric field vector in circular polarization are the same but the phase between them is different. The oscillation direction rotates with time as the electric field propagates with constant amplitude. When looking at the source the electric vector of the wave appears to be rotating counterclockwise, it is called right hand circular polarization. If it appears rotating clockwise, then is the case of left hand circular polarization.

Elliptical polarization consists of two perpendicular electric field components of unequal amplitude and unequal phase [24]. The trace of elliptic polarization, as in circular polarization, rotates either in the left-hand direction or in the right-hand direction, depending on the phase difference. Figure 9 is called *polarization ellipse* and can be expressed in terms of two angular parameters: the orientation angle $\psi(0 \leq \psi \leq \pi)$ and the eccentricity or ellipticity

angle χ ($-\pi/4 < \chi \leq \pi/4$) [25]. The angle ψ is the angle between z-axis and the major axis of the ellipse while the angle χ describes the degree to which the ellipse is oval.

The angle χ is given by (8).

$$\chi = \arctan\left(\frac{b}{a}\right) \quad (8)$$

where a is the length of the semi-major axis of the ellipse and b is the length of the semi-minor axis of the ellipse, as shown in Figure 9.

Linear and circular polarizations are special cases of elliptical polarization. If the major and minor axes of the ellipse are equal ($a = b$), then $\chi = -\pi/4, \pi/4$ and the elliptic polarization becomes the circular polarization. When $b = 0$, then $\chi = 0$ and the trace of the tip of the electric field will be a straight line and the elliptic polarization becomes the linear polarization, with an orientation of 45° .

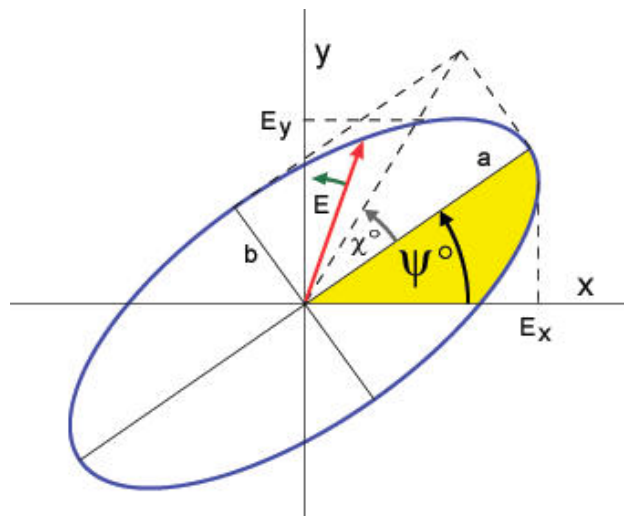


Fig. 9. Polarization ellipse

3.2 Polarization in SAR systems

The antennas of SAR systems are designed to transmit and receive electromagnetic waves of a specific polarization. To create a wave with an arbitrary polarization, it is necessary to have signals with components in two orthogonal or basis polarizations. The two most common basis polarizations in SAR are horizontal linear (H) and vertical linear (V). Circular polarization is used in some applications (for example in weather systems).

In the simpler SAR systems, the antenna is configured in order to use the same polarization in transmission and reception. This traditional kind of radar does not allow determining the complete vector nature of the scattered signal since there is a loss of information regarding the target or the target is completely missed by the radar if the scattered signals have orthogonal sense of polarization. In the more complex systems the antenna is usually designed to transmit and receive waves at more than one polarization (polarimetric radar), which facilitates the complete characterization of the scatterer [26]. A switch is used to direct energy to the different parts of the antenna in sequence, so waves of different polarizations can be transmitted separately (e.g. the H and V parts). Referring to the reception, the antenna is designed to be able to receive the different polarization components of the electromagnetic wave at the same time, because the scatterer can change the polarization of the scattered wave to be different from the incident wave polarization. Those changes in the polarization state of the scattered waves depend upon the characteristic features of the object (scatterer).

A pair of symbols is usually used to denote the transmission and reception polarizations of the system [27]. In the case of a SAR system that uses H and V linear polarizations, the possible channels are the following ones:

- HH: horizontal linear transmission and horizontal linear reception
- HV: horizontal linear transmission and vertical linear reception
- VH: vertical linear transmission and horizontal linear reception
- VV: vertical linear transmission and vertical linear reception

The polarization combinations that use the same polarization in transmission and in reception are called like-polarized (HH and VV). When the transmit and receive polarizations are orthogonal to one another (HV and VH), the combinations are called cross-polarized [28].

According the level of polarization complexity, the SAR system can be classified as [27]:

- Single-polarized: there is a single-polarization transmitted and a single-polarization received (HH or VV or HV or VH imagery).
- Dual-polarized: transmit a horizontally or vertically polarized waveform and measure signals in both polarizations in receive (HH and HV, VV and VH, or HH and VV imagery).

- Full-polarized or quad-polarized: alternate between transmitting H and V polarized waveforms and receive both H and V (HH, HV, VH and VV imagery).

SAR polarimetry extracts more detailed information of targets on land and sea than conventional single-polarized SAR imagery, from the combinations of transmitted and received signals of different polarization states. Polarimetric SAR data is useful for analyzing different scattering processes and for image classification.

3.3 Jones vector

The representation of a plane monochromatic electric field in the form of a Jones vector aims to describe the wave polarization using the minimum amount of information [6].

An electric field vector in an orthogonal basis $(\hat{x}, \hat{y}, \hat{z})$, located in the plane perpendicular to the direction of propagation along \hat{z} can be represented in time domain as (9).

$$\vec{E}(z, t) = \begin{bmatrix} E_{0x} \cos(\omega t - kz + \delta_x) \\ E_{0y} \cos(\omega t - kz + \delta_y) \end{bmatrix} = \text{Re} \left\{ \begin{bmatrix} E_{0x} e^{j\delta_x} \\ E_{0y} e^{j\delta_y} \end{bmatrix} e^{-jkz} e^{j\omega t} \right\} = \text{Re} \{ \underline{\vec{E}}(z) e^{j\omega t} \} \quad (9)$$

For the monochromatic case, the time dependence is neglected. A Jones vector \underline{E} is then defined from the complex electric field vector $\underline{\vec{E}}(z)$ as (10).

$$\underline{E} = \underline{\vec{E}}(z)|_{z=0} = \underline{\vec{E}}(0) = \begin{bmatrix} E_{0x} e^{j\delta_x} \\ E_{0y} e^{j\delta_y} \end{bmatrix} \quad (10)$$

The Jones vector completely defines the amplitude and phase of the complex orthogonal components (in x and y directions) of an electric field. A Jones vector can be formulated as a 2-D complex vector function of the polarization ellipse characteristics as (11) [6]

$$\underline{E} = A e^{j\alpha} \begin{bmatrix} \cos\psi \cos\chi - j \sin\psi \sin\chi \\ \sin\psi \cos\chi + j \cos\psi \sin\chi \end{bmatrix} = A e^{j\alpha} \begin{bmatrix} \cos\psi & -\sin\psi \\ \sin\psi & \cos\psi \end{bmatrix} \begin{bmatrix} \cos\chi \\ j \sin\chi \end{bmatrix} \quad (11)$$

where α is an absolute phase term, ψ is the orientation angle of the polarization ellipse and χ the ellipticity angle of the polarization ellipse, as previously explained.

Table 1 shows the relation of the Jones vector and the parameters of the polarization ellipse for some polarization states.

Polarization state	Unit Jones Vector $\hat{\mathbf{u}}_{(x,y)}$	Orientation angle ψ	Ellipticity angle χ
Linear polarized in the x-direction: Horizontal (H)	$\hat{\mathbf{u}}_H = \begin{bmatrix} 1 \\ 0 \end{bmatrix}$	0	0
Linear polarized in the y-direction: Vertical (V)	$\hat{\mathbf{u}}_V = \begin{bmatrix} 0 \\ 1 \end{bmatrix}$	$\frac{\pi}{2}$	0
Right hand circular polarized (RCP)	$\hat{\mathbf{u}}_R = \frac{1}{\sqrt{2}} \begin{bmatrix} 1 \\ -j \end{bmatrix}$	$\left[-\frac{\pi}{2} \dots \frac{\pi}{2} \right]$	$-\frac{\pi}{4}$
Left hand circular polarized (LCP)	$\hat{\mathbf{u}}_L = \frac{1}{\sqrt{2}} \begin{bmatrix} 1 \\ j \end{bmatrix}$	$\left[-\frac{\pi}{2} \dots \frac{\pi}{2} \right]$	$\frac{\pi}{4}$

Table 1. Jones vectors and the corresponding polarization ellipse parameters for some canonical polarization states

3.4 Scattering or Sinclair matrix

Given the Jones vectors of the incident and the scattered waves, \underline{E}_I and \underline{E}_S , respectively, the scattering process at the target can be represented in terms of these Jones vectors as (12) [6]

$$\underline{E}_S = \frac{e^{-jkr}}{r} S \underline{E}_I \quad (12)$$

where k is the wavenumber and matrix S is the complex 2×2 *scattering* or *Sinclair matrix*.

The term $\frac{e^{-jkr}}{r}$ takes into account the propagation effects both in amplitude and phase. In a fully polarimetric case, a set of four complex images is available. The scattering matrix S represents each pixel in the set and is given by (13)

$$S = \begin{bmatrix} S_{HH} & S_{HV} \\ S_{VH} & S_{VV} \end{bmatrix} \quad (13)$$

where its four elements S_{ij} are referred to as the *complex scattering coefficients*. The diagonal elements of the scattering matrix, S_{HH} and S_{VV} , are called *copolar* elements, since they relate the same polarization for the incident and the scattered fields. The orthogonal to the diagonal

elements, S_{HV} and S_{VH} , are known as *cross-polar* elements since they relate orthogonal polarization states. In monostatic radars, the reciprocity property holds for most targets, so $S_{HV} = S_{VH}$, i.e. the scattering matrix is symmetrical and has only 3 independent elements. Equations 12 and 13 are valid only in the far-field zone where the incident and scattered fields are assumed to be planar.

Different scattering vectors are defined depending on polarization basis. The complex Pauli spin matrix basis set $\{\psi_{4P}\}$ is widely used and is given by (14) [29].

$$\{\psi_{4P}\} = \left\{ \sqrt{2} \begin{bmatrix} 1 & 0 \\ 0 & 1 \end{bmatrix}, \quad \sqrt{2} \begin{bmatrix} 1 & 0 \\ 0 & -1 \end{bmatrix}, \quad \sqrt{2} \begin{bmatrix} 0 & 1 \\ 1 & 0 \end{bmatrix}, \quad \sqrt{2} \begin{bmatrix} 0 & -j \\ j & 0 \end{bmatrix} \right\} \quad (14)$$

The coefficient $\sqrt{2}$ is used to normalize the corresponding scattering vector \underline{k} and to keep the total power invariant, that is $\|\underline{k}\|^2 = \text{Span}(S)$. The scattering vector or covariance vector \underline{k} is a vectorized version of the scattering matrix and is required in order to extract the physical information about the target. For bistatic scattering case, the 4-D \underline{k} -target vector or 4-D Pauli feature vector is given by (15).

$$\underline{k}_4 = \frac{1}{\sqrt{2}} [S_{HH} + S_{VV}, S_{HH} - S_{VV}, S_{HV} + S_{VH}, j(S_{HV} - S_{VH})]^T \quad (15)$$

The scattering matrix S is thus related to the polarimetric scattering target vectors as (16).

$$S = \begin{bmatrix} S_{HH} & S_{HV} \\ S_{VH} & S_{VV} \end{bmatrix} = \frac{1}{\sqrt{2}} \begin{bmatrix} k_1 + k_2 & k_3 - jk_4 \\ k_3 + jk_4 & k_1 - k_2 \end{bmatrix} \quad (16)$$

For monostatic radar case, the 4-D polarimetric target vector reduces to 3-D polarimetric target vector. In this case, the complex Pauli spin matrix basis set $\{\psi_{4P}\}$ results in (17) [30].

$$\{\psi_{3P}\} = \left\{ \sqrt{2} \begin{bmatrix} 1 & 0 \\ 0 & 1 \end{bmatrix}, \quad \sqrt{2} \begin{bmatrix} 1 & 0 \\ 0 & -1 \end{bmatrix}, \quad \sqrt{2} \begin{bmatrix} 0 & 1 \\ 1 & 0 \end{bmatrix} \right\} \quad (17)$$

The 3-D \underline{k} -target vector or 3-D Pauli feature vector is then given by (18).

$$\underline{k}_3 = \frac{1}{\sqrt{2}} [S_{HH} + S_{VV}, S_{HH} - S_{VV}, 2S_{HV}]^T \quad (18)$$

The elements of the 3-D Pauli feature vector, $S_{HH} + S_{VV}$, $S_{HH} - S_{VV}$ and $2S_{HV}$, represent odd reflection, even reflection and multiple reflection respectively [31].

3.5 Coherency matrix

In most geoscience radar applications, the scatterers are generally embedded in a dynamic environment, so they are affected by spatial and/or time variations. These scatterers, called partial scatterers or distributed targets, can no longer be completely described by a scattering matrix S [6]. The concept of coherency matrix was introduced to advance the analysis of partial scatterers in the complex domain [30].

For a reciprocal target matrix, in the monostatic backscattering case, the reciprocity constrains the Sinclair scattering matrix to be symmetrical, so $S_{HV} = S_{VH}$, thus, the 4-D polarimetric coherency $[T_4]$ matrix reduces to 3-D polarimetric coherency matrix $[T_3]$. The 3×3 coherency matrix $[T_3]$ is formed from the outer product of the Pauli scattering vector \underline{k}_3 , as (19) [6] [30].

$$[T_3] = \langle \underline{k}_3 \cdot \underline{k}_3^{*T} \rangle = \left\langle \begin{bmatrix} |k_1|^2 & k_1 k_2^* & k_1 k_3^* \\ k_2 k_1^* & |k_2|^2 & k_2 k_3^* \\ k_3 k_1^* & k_3 k_2^* & |k_3|^2 \end{bmatrix} \right\rangle \quad (19)$$

$$= \frac{1}{2} \begin{bmatrix} \langle |S_{HH} + S_{VV}|^2 \rangle & \langle (S_{HH} + S_{VV})(S_{HH} - S_{VV})^* \rangle & 2\langle (S_{HH} + S_{VV})S_{HV}^* \rangle \\ \langle (S_{HH} - S_{VV})(S_{HH} + S_{VV})^* \rangle & \langle |S_{HH} - S_{VV}|^2 \rangle & 2\langle (S_{HH} - S_{VV})S_{HV}^* \rangle \\ 2\langle S_{HV}(S_{HH} + S_{VV})^* \rangle & 2\langle S_{HV}(S_{HH} - S_{VV})^* \rangle & 4\langle |S_{HV}|^2 \rangle \end{bmatrix}$$

The coherency matrix $[T_3]$ is Hermitian positive semidefinite and contains all the physical information of each pixel.

For the dual-polarization case, each pixel is represented by a 2×2 coherency matrix $[T_2]$ that is obtained from $[T_3]$ by (20).

$$[T_2] = \langle \underline{k}_2 \cdot \underline{k}_2^{*T} \rangle = \left\langle \begin{bmatrix} |k_1|^2 & k_1 k_2^* \\ k_2 k_1^* & |k_2|^2 \end{bmatrix} \right\rangle \quad (20)$$

$$= \frac{1}{2} \begin{bmatrix} \langle |S_{HH} + S_{VV}|^2 \rangle & \langle (S_{HH} + S_{VV})(S_{HH} - S_{VV})^* \rangle \\ \langle (S_{HH} - S_{VV})(S_{HH} + S_{VV})^* \rangle & \langle |S_{HH} - S_{VV}|^2 \rangle \end{bmatrix}$$